International Journal of Pharmaceutics 382 (2009) 151–159

Contents lists available at ScienceDirect

International Journal of Pharmaceutics

journal homepage: www.elsevier.com/locate/ijpharm

Effects of film coating thickness and drug layer uniformity on in vitro drug release from sustained-release coated pellets: A case study using terahertz pulsed imaging

Louise Ho[a,b,c,*], Yvonne Cuppok[d], Susanne Muschert[d], Keith C. Gordon[e], Michael Pepper[b,c], Yaochun Shen[f], Florence Siepmann[d], Juergen Siepmann[d], Philip F. Taday[c], Thomas Rades[a]

[a] School of Pharmacy, University of Otago, P.O. Box 56, Dunedin, New Zealand[1]
[b] Cavendish Laboratory, University of Cambridge, Cambridge CB3 0HE, UK
[c] TeraView Ltd, St. John's Innovation Park, Cambridge CB4 0WS, UK
[d] College of Pharmacy, JE2491, Univ Lille Nord de France, 3 Rue du Professeur Laguesse, 59006 Lille, France
[e] Department of Chemistry and MacDiarmid Institute for Advanced Materials and Nanotechnology, University of Otago, P.O Box 56, Dunedin, New Zealand
[f] Department of Electrical Engineering and Electronics, University of Liverpool, Brownlow Hill, Liverpool L69 3GJ, United Kingdom

ARTICLE INFO

Article history:
Received 21 May 2009
Received in revised form 20 August 2009
Accepted 21 August 2009
Available online 27 August 2009

Keywords:
Controlled release
Coating
Image analysis
Unit operations
Dissolution
Pellets

ABSTRACT

Film coating thickness and terahertz electric field peak strength (TEFPS) were determined using terahertz pulsed imaging (TPI) and employed for the analysis of sustained-release coated pellets (theophylline layered sugar cores coated with Kollicoat® SR:Kollicoat® IR polymer blends). The effects of coating thickness, drug layer uniformity and optional curing were investigated using eight batches of pellets. Ten pellets from each batch were imaged with TPI to analyse the coating morphology (depicted in TEFPS) and thickness prior to release measurements. The results showed TEFPS values of 15.8% and 14.5% for pellets with a smooth drug layer coated at 8.2 and 12.5% (w/w) polymer weight-gain, respectively. Whereas 6.7% was derived for pellets with a coarse drug layer coated at both weight-gains. Although there were major differences in TEFPS, the resulting drug release kinetics were very similar. It was also shown that a 36 μm coating thickness difference was not drug release rate determining. These results suggested that drug release for the pellets studied was not predominately governed by drug diffusion through the polymeric film coating but probably to a large extent limited by drug solubility. TPI proved to be highly suitable to detect non-homogeneities in the drug layer and polymeric film coating.

1. Introduction

Film coating of solid dosage forms is a process commonly performed in order to modify drug release characteristics. Sustained-release film coating is frequently applied onto spherical pellets to be incorporated into capsules or compressed into tablets. In comparison to single-unit dosage forms, pellets offer the advantage of allowing the drug to spread throughout the gastrointestinal track more evenly and thus providing a more predictable gastric transit time and drug absorption. This consequently improves the therapeutic effects of a medical treatment, when the drug release is well controlled from film coated pellets, delivering a predictable amount of drug within the therapeutic range for a prolonged period of time (Nitz and Taranto, 2008; Bechgaard and Nielsen, 1978). Generally, the drug release rate of sustained-release pellets is predominately affected by the film coating thickness and film quality (Haddish-Berhane et al., 2006).

To date, the product design and development of new multiparticulate systems are still largely carried out in an empirical manner, with the film coating thickness and quality of the coated pellets being expressed in terms of polymer weight-gain (Ringqvist et al., 2003). For pellets like the ones used in this study, which consisted of a sugar starter core, a drug layer and polymeric coating layer on top; not only is coating polymer weight-gain a relatively non-specific measurement (Ho et al., 2008, 2009) but also the film coating thickness uniformity of a pellet is quite often related to undulations of the drug layer underneath, and weight-gain does not reflect this information (Heinicke and Schwartz, 2007). Apart from mechanistic studies on drug release using in vitro release measurements (Shao et al., 2002; Muschert et al., 2009; Dashevsky et al., 2005; Siepmann et al., 2008, 2007), a range of analytical techniques including atomic force microscopy (Ringqvist et al., 2003), nuclear magnetic resonance spectroscopy (NMR) (Ensslin et al., 2008), electron paramagnetic resonance spectroscopy (EPR) (Ensslin et al.,

* Corresponding author at: School of Pharmacy, University of Otago, P.O. Box 56, Dunedin 9054, New Zealand. Tel.: +64 3479 7275; fax: +64 3479 7034.
E-mail address: louise.ho@otago.ac.nz (L. Ho).
[1] http://www.otago.ac.nz/pharmacy.

0378-5173/$ – see front matter © 2009 Elsevier B.V. All rights reserved.
doi:10.1016/j.ijpharm.2009.08.025

2009), energy dispersive X-ray imaging (EDX) (Ensslin et al., 2008), Raman microimaging (Ringqvist et al., 2003), scanning electron microscopy (SEM) (Heinicke and Schwartz, 2007; Johansson and Alderborn, 2001) and fluorescence microscopy (Andersson et al., 2000) have been employed to investigate the physical characteristics of the film coating on pellets to gain a better understanding of their effect on the release behaviour.

Terahertz pulsed imaging (TPI) was recently introduced into the pharmaceutical field (Fitzgerald et al., 2005), mainly for the analysis of solid dosage forms. Operating in the far-infrared region of the electromagnetic spectrum (2–120 cm^{-1}), most pharmaceutical excipients are transparent or semi-transparent to the terahertz radiation. This allows for an unparalleled axial penetration depth of approximately 5 mm. Owing to advances in semi-conductor device development, ultra-short pulses of the terahertz radiation can now be easily generated without the need of cryogenic cooling. The core technology and the way in which the terahertz radiation is generated and detected is essentially the same between the spectroscopy set-up and the imaging set-up. An ultrafast (75 fs), Ti-sapphire laser beam in the NIR range (800 nm) is split into two: the probe beam and the pump beam. Both the terahertz emitter and detector are photoconductive, gallium arsenide (GaAs) semi-conductors. Electron–hole pairs are generated when the pump beam irradiates the surface of the GaAs emitter. These electron–hole pairs are then separated and accelerated by a direct current (DC) electric field across the emitter, which results in a change in the current density (Pickwell and Wallace, 2006). This change in the electric dipole leads to the generation of a terahertz pulse that emits into free space on a sub-picosecond timescale. The emitted terahertz pulse is inherently broadband and coherent. For TPI, once the terahertz pulse is reflected off the sample it is then coupled from free space and focused onto the back of the GaAs detector. The detection method is essentially in reverse of the terahertz emission process; except the role of the external DC electric field applied is now replaced by the arrival of the terahertz pulse. The process is optically gated as the NIR laser probe beam is time delayed against the arrival of the terahertz pulse. By shining the NIR laser probe beam onto the electrode gaps on the detector, electron–hole pairs are generated at the front surface of the GaAs substrate (Zeitler et al., 2007c). At the same time, the arrival of the terahertz pulse accelerates the electrons across the detector substrate. This change in the photocurrent between the electrodes with time is measured using the delay between the terahertz pulse and the laser probe beam. Thus a terahertz signal/waveform as a function of time is formed (Taday and Newnham, 2004). This time domain waveform holds both phase and amplitude information hence both absorption coefficient and refractive index can be derived (Taday and Newnham, 2004). It is also possible to deconvolve the raw terahertz waveform and derive terahertz parameters such as terahertz electric field peak strength (TEFPS), which is related to the physicochemical properties of the film coating and/or solid dosage form under investigation (Shen and Taday, 2008; Ho et al., 2008).

Solid dosage forms such as tablets (with or without coating) and capsules (soft or hard gelatine) have been investigated with TPI (Zeitler et al., 2007c,b), and revealed internal structures that were previously accessible only from destructive measurements. Film coating thickness of tablets in particular was studied to investigate thickness uniformity and thickness variations within the batch for sustained-release coated tablets (Ho et al., 2007). The terahertz parameter, TEFPS was employed to investigate a film coating process scale-up failure (Ho et al., 2008). Both coating thickness and TEFPS were found to be indicative of the subsequent dissolution performance of tablets with a modified-release film coating (Spencer et al., 2008; Ho et al., 2009). Moreover, using terahertz parameters the tablet central band was identified as the film coating 'weak spot' on round, biconvex tablets (Ho et al., in press-b). It was observed that the coating thickness around the tablet central band domain was significantly lower, with lower film coating density and higher surface roughness (hence higher specific surface area exposed to the dissolution medium) when compared to that on the top and bottom domain on biconvex tablets (Ho et al., in press-b). Results from conventional dissolution testing confirmed that drug release from the central band was faster than release from the top and bottom surfaces (Ho et al., in press-b). As the terahertz parameters are directly derived from the time domain waveform, a multivariate analysis study employing a PLS model built from the deconvolved waveform and the mean dissolution time (MDT) of the tablets was used to predict drug dissolution of two more batches of tablets coated with the same process parameters (Ho et al., in press-a). Developing from our previous studies on coated tablets, in this work we used TPI to gain information on the film coating surface morphology and thickness in attempt to explore the effects of film coating thickness, drug layer uniformity and curing on drug release from sustained-release coated pellets.

2. Materials and methods

2.1. Materials

The following materials were used in this study: theophylline monohydrate (BASF, Ludwigshafen, Germany); nonpareil sugar starter cores (diameter = 3.9 mm, Boiron, Lyon, France); poly(vinyl acetate) (Kollicoat® SR 30 D; BASF, Ludwigshafen, Germany), poly(vinyl alcohol)-poly(ethylene glycol) graft copolymer (PVA-PEG graft copolymer, Kollicoat® IR; BASF); triethyl citrate (TEC; Morflex, Greensboro, USA); sucrose (Beghin Say, Thuleries, France); talc (Luzenac Val Chisone, Porte, Italy). The average particle size of theophylline monohydrate was determined using optical microscopy (Axioskop, CarZeiss Inc., Jena, Germany).

2.2. Preparation of coated pellets

Eight batches of pellets were produced to investigate the effects of varying coating thickness, drug layer uniformity and curing on drug release from sustained-release pellets. Details of the pellet design specifications for each of the batches are summarized in Table 1. The average diameters from 10 samples per batch, obtained with a digital vernier caliper (Kincrome Australia Pty. Ltd., Victoria, Australia) are also included in Table 1. Sugar starter cores were coated with aqueous mixture of theophylline (10% (w/w) suspension) and sucrose (52% (w/w) solution) in a pan coater (AR400 equipped with a UC pan, Erweka, Le Bec Hellouin, France) using a spray gun (DeVilbiss GFG 502, ITW Surfaces et Finitions, Valence, France) until a drug loading of 10% ((w/w) based on the core weight) was achieved. The process parameters were as follows: inlet temperature = 60 °C; product temperature = 30–35 °C;

Table 1
A summary of the four batches of sustained-release pellets coated for this study.

Sustained-release pellet batches	Batch I	Batch II	Batch III	Batch IV	Batch V	Batch VI	Batch VII	Batch VIII
Drug layer	Smooth	Smooth	Coarse	Coarse	Smooth	Smooth	Coarse	Coarse
Film coating level	8.2%	12.5%	8.2%	12.5%	8.2%	12.5%	8.2%	12.5%
Curing	No	No	No	No	Yes	Yes	Yes	Yes
Average diameter/mm (n = 10)	5.7	6.3	5.9	6.0	5.7	6.1	5.8	6.0

pan rotation speed = 20 rpm; spray rate = 1–3 g/min; atomization pressure = 1.2 bar; nozzle diameter = 1.5 mm. The surface of the drug loaded cores produced using this method was coarse, thus this type of drug loaded cores was used to coat pellets for batches III, IV, VII and VIII (Table 1). For a smooth drug layer, the coarse drug loaded cores were further spheronised for 180 s at 750 rpm (Caleva model 15; Caleva, Dorset, UK) prior to the film coating process for batches I, II, V and VI (Table 1). During spherionization, small amounts of water were sprinkled onto the drug loaded cores, which were subsequently dried for 24 h at room temperature. There was no significant weight loss as the result of the spherionization step. 25 drug loaded cores were sampled pre-spherionization and another 25 samples were taken post-spherionization and weighed. The average weight of the drug loaded cores pre-spherionization was 146 ± 15 and 148 ± 14 mg for post-spherionization. A two-tailed, unpaired *t*-test was performed and a *P*-value of 0.55 was calculated ($\alpha = 0.05$).

Drug loaded cores were coated with a blend of Kollicoat® SR 30 D [an aqueous polyvinyl acetate (PVAc) dispersion] and Kollicoat® IR [polyvinyl alcohol–polyethylene glycol (PVA-PEG) graft copolymer]. The blend ratio was 75:25 ((w/w) referring to the dry masses). The aqueous PVAc dispersion Kollicoat® SR 30 D (30% (w/w) solids content, referred to the total dispersion mass) was plasticized overnight with triethyl citrate (5% (w/w) based on the polymer content). 30 min prior to the application of the coating formulation, appropriate amounts of the 10% (w/w) aqueous PVA-PEG graft copolymer solution as well as 1.5% ((w/w) based on the total solids content) talcum were added and the dispersion was gently stirred throughout the coating process. All drug loaded cores were coated in a drum coater (Hi Coater HCT 30 mini, Loedige, Paderborn, Germany) until a weight-gain of 8.2% (for batches I, III, V and VII) and 12.5% (for batches II, IV, VI and VIII) was achieved (equivalent to 10.9 and 16.6 mg/cm^2, respectively). The process parameters were as follows: inlet temperature = 60 °C; product temperature = 35 ± 3 °C; pan rotation speed = 25 rpm; spray rate = 2–3 g/min; atomization pressure = 1.25 bar; nozzle diameter = 0.8 mm. After coating the pellets were further fluidized for 10 min and batches V–VIII were cured for 24 h at 60 °C in an oven.

2.3. Terahertz pulsed imaging

Ten pellets from each batch were randomly sampled and imaged individually using a TPI Imaga2000 (TeraView Ltd., Cambridge, UK). The morphology of each pellet was modeled in front of a 670 nm laser gauge prior to scanning with the terahertz beam. The imaging process was fully automated; the six-axis robotic arm ensured the surface of the pellet was always presented at normal angle to the terahertz beam. The instrument was set-up to allow for 5 mm axial penetration depth in air, while the mapping step-size (point-to-point mode) was set at 100 μm, scanning within a circular area of 3 mm radius.

Both coating thickness and TEFPS were determined for each pixel and an average value over the sampled area (around 2500 pixels for a circular area of 3 mm radius) was calculated for each pellet. Coating thickness (in μm) was derived directly using the following equation: $2d_{coat} = \Delta tc/n$. Where d_{coat} is the coating thickness, Δt is the time delay between the terahertz reflections, c is the speed of light and n is the refractive index of the coating matrix (Ho et al., 2007). The refractive index of the film coating was obtained using terahertz pulsed spectroscopy in transmission mode, and was found to be 1.5 (Ho et al., 2007) and 1.83 for sucrose and that of theophylline monohydrate was 1.85 (Zeitler et al., 2007a). The refractive index value of 1.5 was used for the coating thickness calculations and a value of 1.83 ($1.85 \times 16\% + 1.83 \times 84\%$) for the drug layer thickness calculations (the drug layer contained 16% of theophylline monohydrate and 84% of sucrose). TEFPS provides information on the degree of surface roughness and relative density of the film coating. It measures the magnitude of the reflected terahertz pulse from the pellet surface normalised to that of the initial pulse (Ho et al., 2008) and is expressed as a percentage value (%). There was no significant terahertz signal loss as a result of the curvature of the pellets. The TEFPS per pixel was determined and the values were comparable to those obtained from tablet central bands for our previous studies employing biconvex tablets (Ho et al., 2009, in press-a, in press-b).

2.4. Drug release measurements and comparisons

Post mapping with TPI, the same pellets were used for drug release measurements in 900 mL of phosphate buffer pH 7.4 (USP 30), using the paddle apparatus (Sotax AT 7, Basel, Switzerland). Temperature was maintained at 37 °C and a paddle speed of 100 rpm was used. An online UV–visible spectrophotometer (Beckman DU 650, Beckman Coulter, Villepinte, France) was employed to determine the drug concentration in solution at a detection wavelength of 271 nm. Samples were collected at the following time intervals up to 1.5 h: 0, 0.25, 0.5, 0.75, 1, and 1.5 h, then hourly over 24 h thereafter. An average drug release profile was derived from ten pellets for each batch to compare the in vitro drug release characteristics.

To compare the dissolution profiles of the various pellet batches formulated, a model independent approach employing the similarity factor (f_2) was carried out in accordance with FDA guidelines, as it describes similarity between the average release profile (in % drug dissolved) of the reference-set and the test-set (Food and Drug Administration, 1997). The similarity factor is calculated from the equation below, and it is a logarithmic transformation of the sum of squared differences between the reference-set drug release values at time t (R_t) and the test-set drug release values at time t (T_t), where n is the number of sampling time points (in the current study $n = 29$) (Moore and Flanner, 1996).

$$f_2 = 50 \log \left\{ \left[1 + \frac{1}{n} \sum_{t=1}^{n} (R_t - T_t)^2 \right]^{-0.5} \times 100 \right\}$$

An f_2 value of 100 means the average release profile from the test-set is identical to the average dissolution profile of the reference-set, and as the f_2 value draws closer to 0 the difference between the two dissolution curves gets greater. The similarity factor (f_2) is widely employed in the pharmaceutical industry for testing the equivalence between two in vitro drug release curves (Graffner, 2006), and has been included as one of the in vitro assessment criterions by both the FDA and EMEA (Costa, 2001). Apart from immediate release dosage forms, the similarity factor test has also been applied to modified-release dosage forms (European Agency for the Evaluation of Medicinal Products, 1999; Malaterre et al., in press). Both the FDA and EMEA stated in their guidelines that two drug release profiles are deemed similar if the f_2 value lies between 50 and 100 (Food and Drug Administration, 1997; European Agency for the Evaluation of Medicinal Products, 1999). In this study, the similarity factor test was applied to assess drug release as a function of changes in the film coating thickness, drug layer uniformity and curing.

2.5. Scanning electron microscopy and stereo-microscopy imaging

To examine the morphology of the drug and film coating layer, scanning electron microscopy (SEM, FEI Philips XL30 sFEG, Philips Electron Optics) images were obtained for one pellet from each

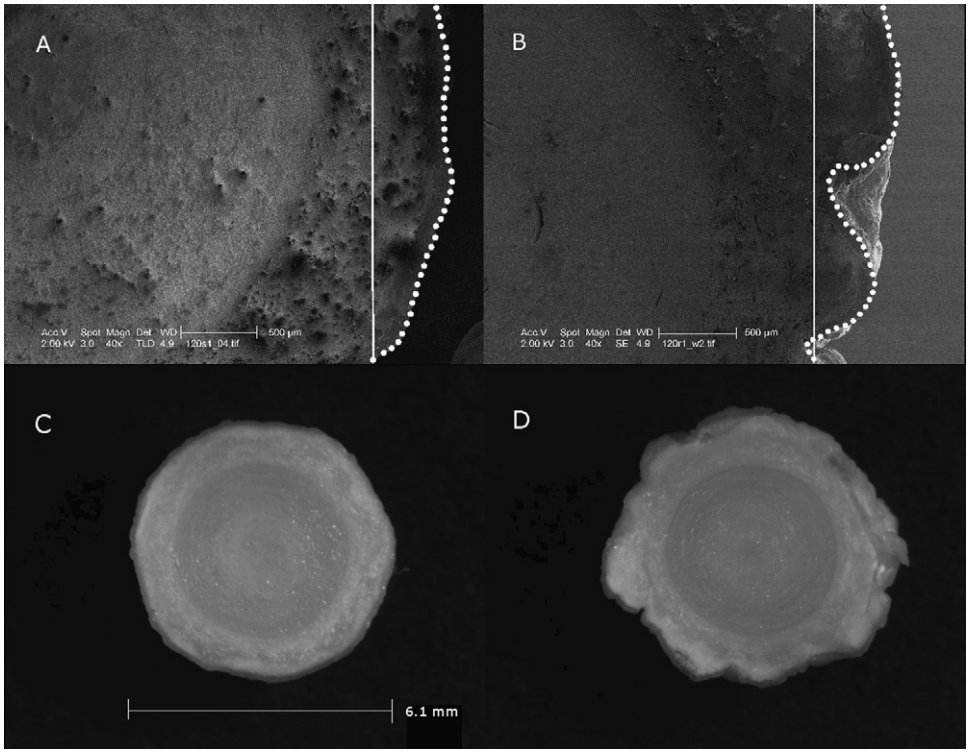

Fig. 1. Cross-section, SEM micrographs of pellets from batch II (A) and IV (B), with their respective global images presented in (C) and (D). Each of the three main compartments of the pellet is clearly visible: the starter core, the drug layer and the film coating layer. The surface morphology of the film coating on the pellet in (A) is smoother than on the pellet in (B), with a R_a value of 1.09 and 1.33, respectively.

batch. Micrographs of the film coating surface and the pellet cross-sections were imaged at magnifications of 40×, 150× and 300×. Surface roughness factors (R_a) for the various pellets were calculated from the cross-sectional images taken at 40× (Ho et al., in press-b). R_a is the ratio of the distance tracing the surface morphology over the sampled distance, the higher the R_a the coarser the surface morphology (Fig. 1). Furthermore, Feret's Diameter for coating droplet deposits on the surface of the pellet were measured from SEM micrographs taken at 40× magnification in order to determine the effect of surface roughness on TEFPS. Due to the droplet irregularity in both size and shape, the diameter length was obtained in both the x and y directions from 10 coating droplet deposits per pellet. The global images of the pellet cross-sections were obtained using a stereo-microscope (Nikon SM2800, Nikon Instruments Ltd., Melville, USA) fitted with a digital camera (Moticam 1000, Motic Ltd., Xiamen, China). These images were taken at 20× magnification.

3. Results and discussion

3.1. Sustained-release pellets

All pellets consisted of three main compartments: the starter core, the drug layer and the film coating (Fig. 1). The surface morphology of the film coating layer varied as a function of the uniformity of the drug layer underneath the film coating layer and the R_a was calculated to quantify the morphological difference between batches I and III, and batches II and IV. The R_a for a pellet coated at 8.2% (w/w) polymer weight-gain on a smooth drug layer was 1.09 (batch I) and 1.21 for a pellet with a film coating on the coarse drug layer (batch III). Furthermore, for a pellet coated at 12.5% (w/w) polymer weight-gain, a R_a of 1.09 was measured from the film coating on a smooth drug layer (batch II) and 1.33 from the film coating on a coarse drug layer (batch IV).

At 10% (w/w) drug loading, the drug layer has a thickness of around 1 mm. The interface between the drug layer and the starter core was clearly visible in the TPI B-scan (Fig. 2). Similar to an ultrasound B-scan (Shen and Taday, 2008), a TPI B-scan is a virtual cross-sectional slice of the imaged pellet. Using pellets from batches I and II as an example, a distinctive light blue band was visible in the TPI B-scan images, at a terahertz penetration depth corresponding to 1.6 ± 0.1 mm (Fig. 2). This is the drug layer/starter core interface. Since the refractive index of the coating layer and drug layer in the sample is 1.67 ± 0.17, the 1.6 mm terahertz penetration depth in air equates to 0.96 ± 0.1 mm penetration depth in a tablet. Hence the TPI B-scans in the depth direction show that the thickness of the drug layer is approximately 1 mm (Fig. 2). Other interfaces are also depicted in the TPI B-scans, where the air/film coating interface is shown in red and the film coating/drug layer interface immediately beneath pellet surface is displayed as the lighter blue band. It is interesting to note that there are additional interfaces within the drug layer detected in the TPI B-scan. These interfaces are a direct result of the drug layering process, which was carried out in a pan coater. There were drying intervals throughout the drug layering procedure, during which the drug layer was allowed to dry for approximately 2–3 min before layering more drug solution on the surface of the starter cores, and this was repeated until the target drug loading was reached. Each time the spraying process was interrupted, it resulted in a density change within the drug layer, which was detected as a change in the refractive index. These changes in the refractive index were discerned as interfaces within the drug layer and were visible in the terahertz B-scans (Fig. 2).

3.2. Variations in film coating thickness (batch I vs. batch II)

Results on the film coating thickness measurements using TPI for batches I and II are detailed in Table 2. The TPI images showed that at 8.2% (w/w) film coating weight-gain (batch I), the average

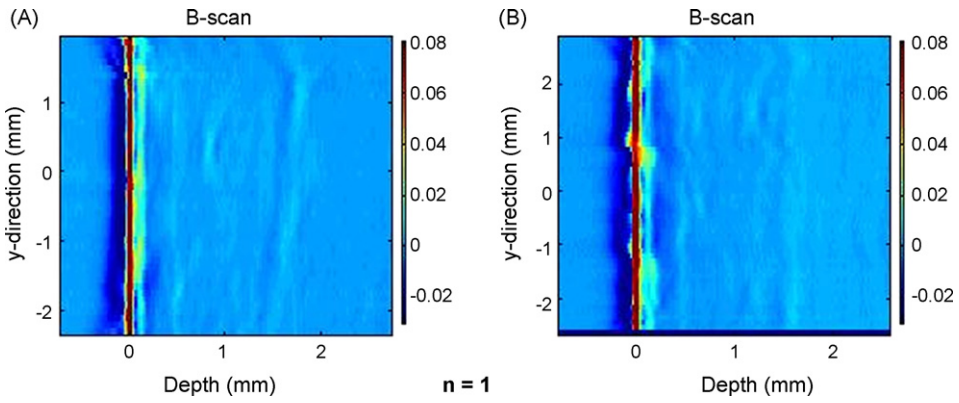

Fig. 2. Terahertz B-scan images of a pellet from batch I (A) and batch II (B). These are cross-sections in the depth direction, where the red band is the air/film coating interface, the lighter blue band that immediately follows is the film coating/drug layer interface, and the thicker light blue band at around 1.5 mm in terahertz penetration depth is the drug layer/starter core interface. The colour scale bar indicates the height of the terahertz signal in a.u. The curvature of the film coating is offset for clarity. (For interpretation of the references to colour in this figure legend, the reader is referred to the web version of the article.)

film coating thickness for smooth pellets was 66 and 102 μm for pellets coated at 12.5% (w/w) (batch II). A two-tailed, unpaired *t*-test was performed, producing a *P*-value of 0.0002; indicating a statically significant coating thickness difference between the two batches (null hypothesis, $\alpha = 0.05$). The coating thickness for batch I ranged from 48 to 99 μm, whereas it ranged between 82 and 135 μm for batch II. These coating thickness ranges highlighted the large extent of coating variability within the batch (Table 2). Interestingly, despite a coating thickness difference of 36 μm between batches I and II, no significant differences were observed in the drug release profiles (Fig. 3), with a f_2 value of 87. This indicated that the particular formulation used in this study is robust with respect to variations in the film coating thickness, which may constitute a major advantage from a practical point of view in formulation. Moreover, the results may also suggest that the rate of drug release was not solely governed by the rate of drug diffusion through the polymeric coating layer.

Drug release profiles from batches I and II both exhibit a lag-time of approximately 2 h, followed by an approximately zero order theophylline drug release (Fig. 3). Upon contact with the dissolution medium, water penetrates into the PVAc/PAV-PEG polymeric layer (Strübing et al., 2007). The osmotic activity of the sugar core is one of the major driving forces behind a continuous water influx, which can be expected to hinder the diffusion of dissolved drug through the membrane in the opposite direction. This phenomenon was also detected using nuclear magnetic resonance (NMR) in a study by Ensslin et al., in which a 'one way stream' of dissolution medium into the pellet though a PVAc/PVA-PEG film was suggested during the drug dissolution lag-time (Ensslin et al., 2008). The fact that an approximate zero order drug release kinetics were observed once theophylline release started might be attributed to the relatively low solubility of the theophylline [12 mg/mL in phosphate buffer, pH 7.4 at 37 °C (Muschert et al., 2009)] and the limited amount of free water available for drug dissolution within the pellets. As a result, a saturated theophylline solution can be expected to exist at the inner face of the film coating surface. Since perfect sink conditions were maintained throughout the dissolution experiments, the driving force of drug diffusion for the pellets investigated in this study was constant. Thus the theophylline release rate was time-independent, as long as a saturated drug solution was provided at the inner face of the film coating surface.

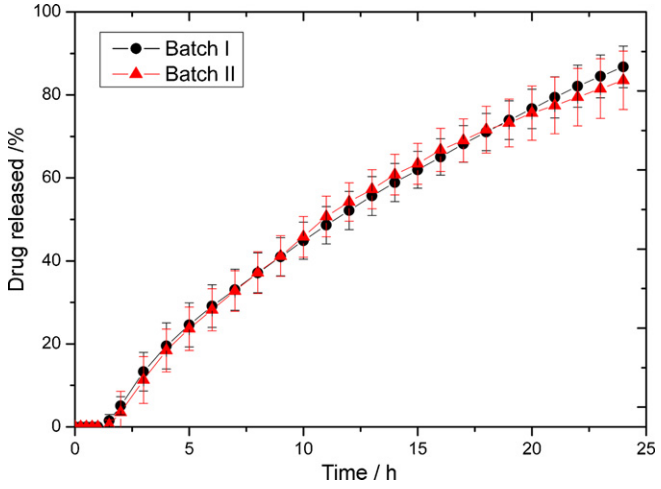

Fig. 3. Average drug release profiles of all 10 pellets from batch I (black circle) and batch II (red triangle) taken over the 24 h period. The average coating thickness difference between the two batches was 36 μm, which resulted in no obvious difference in the release profiles. .

3.3. Drug layer uniformity and film coating surface morphology

Drug layer uniformity is generally presumed to affect the overall film coating surface morphology, thus rendering a 'critical coating level' necessary to cover the undulations in the drug layer underneath the film coating, to avoid failure in achieving modified drug release attributed to areas with very thin coatings (Heinicke and Schwartz, 2007). In this study, sugar starter cores were layered with theophylline particles with an average diameter of 77 ± 32 μm, consequently the surface of the resultant drug loaded cores was very coarse. These drug-loaded cores were either directly coated with a PVAc/PVA-PEG film (batches III and IV) or spheronised prior to coating to achieve a smoother drug layer (batches I and II) (Fig. 4). A degree of smoothing occurred subsequent to the application of the PVAc/PVA-PEG film coating, this was more apparent with pellets from batches III and IV than batches I and II (Fig. 1). Nevertheless, clear differences in the surface morphology were still visible between pellets with a spheronised drug-loaded core/smooth drug layer (batches I and II) and those with a coarse drug layer (batches III and IV) (Fig. 5).

TEFPS values derived from the TPI maps provide information on the surface morphology and also revealed major differences between batches I and III and batches II and IV. The average TEFPS value for batch I was 15.8% whereas it was 6.7% for batch III. Similarly, an average TEFPS of 14.5% was derived for batch II as opposed to 6.7% for batch IV. The lower the TEFPS the higher the film coating surface roughness or in the case of this study the coarser the

Table 2
Terahertz measurements on TEFPS and coating thickness for all batches are presented here. There was no statistically significant difference in the physical characteristics between cured and uncured pellet film coatings, as all Student *t*-test *P*-values were above the null-hypothesis ($\alpha = 0.05$).

Uncured	TEFPS (%)	Coating thickness (μm)	Cured	TEFPS (%)	Coating thickness (μm)
Batch I_S1	16.1	77	Batch V_S1	16.2	94
Batch I_S2	15.7	72	Batch V_S2	16.3	59
Batch I_S3	17.1	50	Batch V_S3	16.7	70
Batch I_S4	14.7	51	Batch V_S4	14.8	66
Batch I_S5	16.7	80	Batch V_S5	16.3	86
Batch I_S6	15.8	49	Batch V_S6	17.6	70
Batch I_S7	14.5	78	Batch V_S7	16.8	42
Batch I_S8	15.9	48	Batch V_S8	17.2	66
Batch I_S9	16.4	99	Batch V_S9	15.8	90
Batch I_S10	15.2	52	Batch V_S10	14.1	53
Average	15.8	66	Average	16.2	70
SD	0.8	18	SD	1.1	16
Student's *t*-test	0.408	0.602			
Batch II_S1	15.8	101	Batch VI_S1	14.6	100
Batch II_S2	16.1	135	Batch VI_S2	15.4	78
Batch II_S3	15.3	104	Batch VI_S3	15.2	95
Batch II_S4	13.4	85	Batch VI_S4	15.4	79
Batch II_S5	14.9	94	Batch VI_S5	15.7	83
Batch II_S6	13.3	82	Batch VI_S6	15.2	95
Batch II_S7	13.6	90	Batch VI_S7	15.0	106
Batch II_S8	14.0	117	Batch VI_S8	15.1	93
Batch II_S9	13.9	98	Batch VI_S9	15.8	118
Batch II_S10	14.3	116	Batch VI_S10	14.2	86
Average	14.5	102	Average	15.2	93
SD	1.0	17	SD	0.5	13
Student's *t*-test	0.0928	0.273			
Batch III_S1	6.8	51	Batch VII_S1	7.0	66
Batch III_S2	6.6	71	Batch VII_S2	5.8	53
Batch III_S3	6.3	54	Batch VII_S3	6.8	14
Batch III_S4	5.7	49	Batch VII_S4	7.7	54
Batch III_S5	7.0	65	Batch VII_S5	6.8	42
Batch III_S6	6.5	65	Batch VII_S6	6.6	61
Batch III_S7	6.1	55	Batch VII_S7	7.9	67
Batch III_S8	7.0	55	Batch VII_S8	6.9	61
Batch III_S9	6.6	67	Batch VII_S9	7.8	52
Batch III_S10	7.9	86	Batch VII_S10	6.5	50
Average	6.7	62	Average	7.0	52
SD	0.6	11	SD	0.6	15
Student's *t*-test	0.380	0.145			
Batch IV_S1	6.6	78	Batch VIII_S1	6.5	79
Batch IV_S2	6.8	76	Batch VIII_S2	6.3	51
Batch IV_S3	5.9	66	Batch VIII_S3	7.0	74
Batch IV_S4	5.5	60	Batch VIII_S4	7.0	85
Batch IV_S5	6.4	68	Batch VIII_S5	5.6	52
Batch IV_S6	8.9	127	Batch VIII_S6	6.8	74
Batch IV_S7	7.4	83	Batch VIII_S7	6.4	71
Batch IV_S8	5.0	47	Batch VIII_S8	6.2	72
Batch IV_S9	8.0	90	Batch VIII_S9	6.8	72
Batch IV_S10	7.1	90	Batch VIII_S10	7.4	91
Average	6.7	78	Average	6.6	72
SD	1.2	22	SD	0.5	13
Student's *t*-test	0.723	0.428			

surface morphology (Ho et al., in press-b). This was further confirmed with the Feret's Diameter obtained from the coating droplet deposits on the surface of the pellets. The results are shown in Table 3, where all droplet depositions are of the size range that is comparable to the wavelength of the terahertz radiation (83 μm to 5 mm) and can cause signal scattering (Shen et al., 2008). With a coarser surface, the surface area available for the penetration of the dissolution medium is also higher (Ho et al., in press-b). In our previous study, we observed variations in the surface morphology and more specifically surface roughness was an important factor for drug release from sustained-release tablets (Ho et al., in press-b), Rohera et al. also found that a higher film coating surface roughness resulted in a faster drug release rate (Rohera and Parikh, 2002). However, when comparing the drug release results from batch III with batch I, the average drug release curve from batch III was similar to that of batch I (Fig. 6A), with a f_2 value of 75. The average drug release curves were also similar between batches II and IV (Fig. 6B), and the f_2 value was 87 for these two batches. This again highlights the robustness of the formulation investigated in the present study and reinforces the hypothesis on the critical importance of the limited drug solubility on the control of drug release as even major differences in the film coating roughness did not significantly affect the resulting drug release rate.

Table 3
The average Feret's Diameters (in the *X* and *Y* directions) of droplet depositions on pellet surfaces are presented here. One pellet was sampled from each batch and imaged with the SEM. Ten droplets per pellet were then measured. The diameter range for both the X and Y directions are also depicted.

Droplet deposition	Batch I (μm)		Batch II (μm)		Batch III (μm)		Batch IV (μm)	
	X direction	*Y* direction	*X* direction	*Y* direction	*X* direction	*Y* direction	*X* direction	*Y* direction
Average (n = 10)	188.82	178.34	173.54	135.12	250.7	253.2	193.62	204.16
Minimum	89	105	94	80	112	120	119	109
Maximum	311	279	361	263	366	437	370	352

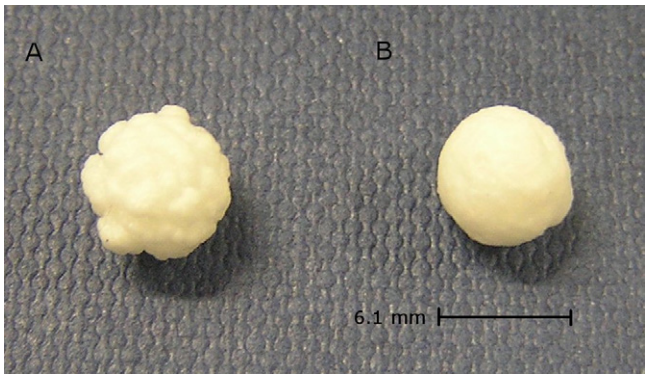

Fig. 4. Pellet produced from a coarse drug-loaded core directly coated with the PVAc/PAV-PEG film without further spheronisation of the drug layer (A). Pellet coated after spheronisation of the drug-loaded core produced, showing a smoother surface morphology (B).

The coating thickness variation as a result of changes in the drug layer uniformity was indicated in the coating thickness standard deviation for each pellet. The coating thickness measured using TPI for each sample was detected over 2500 pixels for an area of 27 mm^2 (based on a circle of 3 mm radius). The average coating thickness variation over the 2500 pixels was 19 μm for batch I, whilst it was much higher (57 μm) for batch III. Similarly the average coating thickness standard deviation over the 2500 pixels was 19 μm for batch II and the variation was much higher for the coarse film coating batch IV at 78 μm. Furthermore, the coating thickness measurements from the terahertz images showed that the coating thickness for the pellets with a smooth drug layer (and hence a smooth film coating, batches I and II) was higher than the film coating thickness on pellets with a coarse drug layer (and hence a coarse film coating layer, batches III and IV). The average film coating thickness for batch I was 66 μm as opposed to 62 μm for batch III, and the average coating thickness for batch II was 102 μm compared to 78 μm for batch IV. The terahertz coating thickness maps showed that the coating thickness in the valleys was lower than that on the peaks, indicating that the growth of the film coating

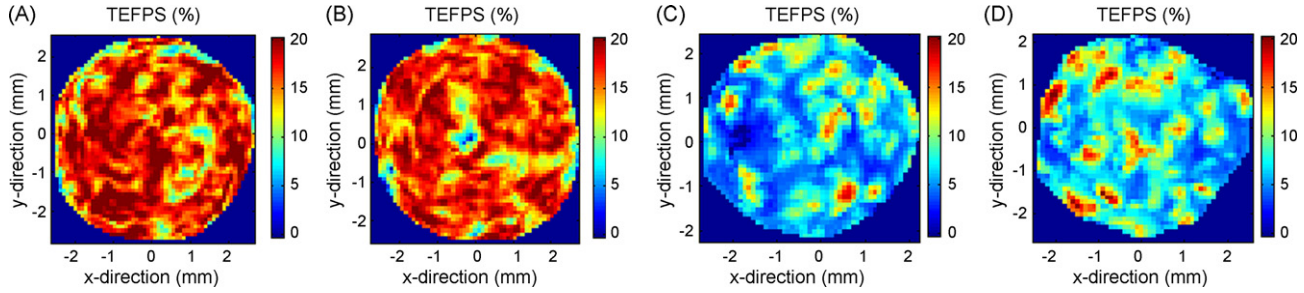

Fig. 5. TEFPS, 2D maps of a pellet from batch I (A), batch II (B), batch III (C) and batch IV (D). The film coating surface roughness in (A) and (B) was lower than the film coating surface roughness in (C) and (D). The colour bar is in %. (For interpretation of the references to colour in this figure legend, the reader is referred to the web version of the article.)

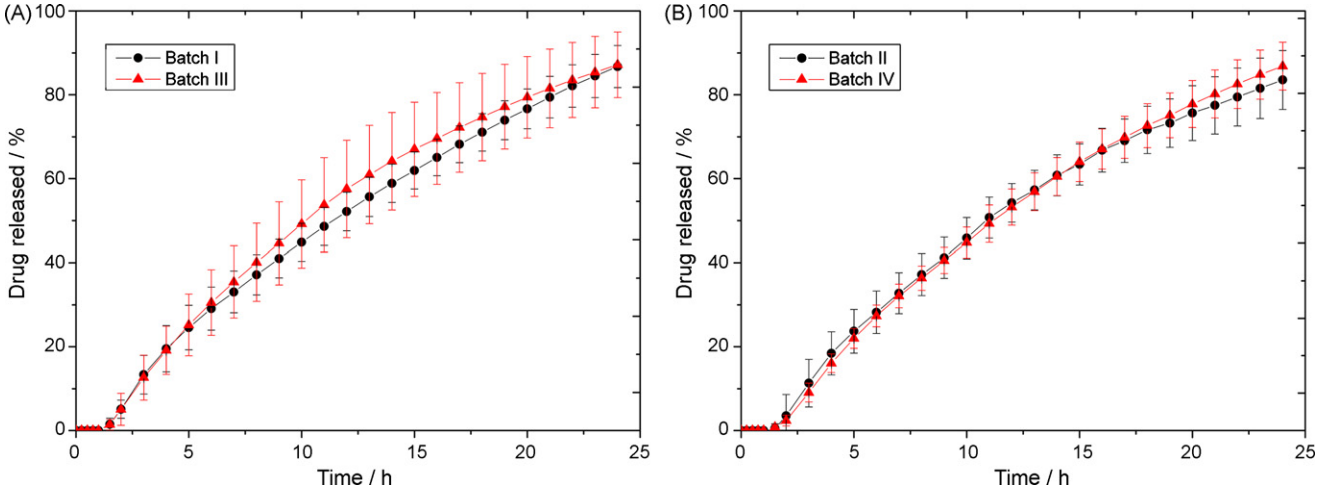

Fig. 6. Comparison between the average drug release profiles of 10 pellets from batch I (black circle) and batch III (red triangle) (A). Average dissolution profile of 10 pellets from batch II (black circle) and batch IV (red triangle) (B).

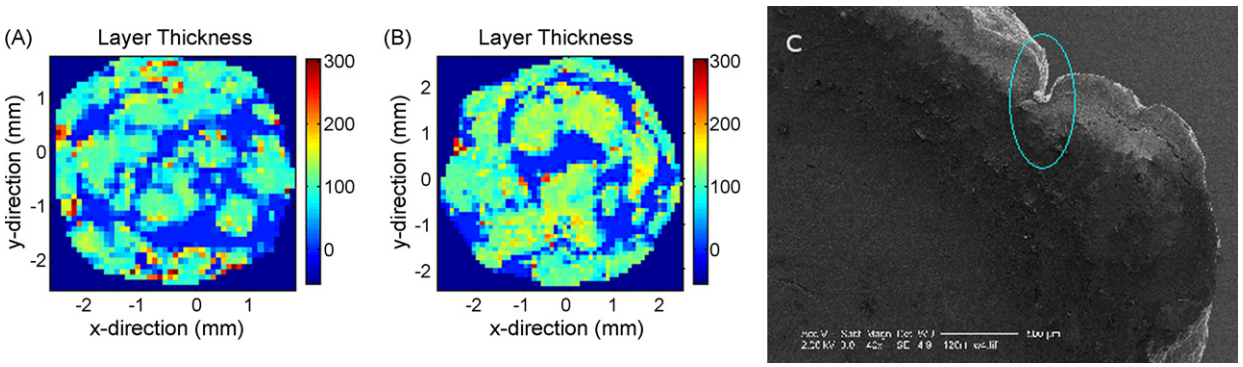

Fig. 7. Images (A) and (B) are coating thickness 2D maps of a pellet from batch III (A) and batch IV (B). The colour scale is in μm. There are areas of very thin coating, particularly in the 'valleys' of the film coating. This is also depicted and confirmed with the SEM micrograph (C), where the coating thickness in the 'valleys' (indicated by an ellipse) of the film coating structure is much thinner than that on the 'peaks'. (For interpretation of the references to colour in this figure legend, the reader is referred to the web version of the article.)

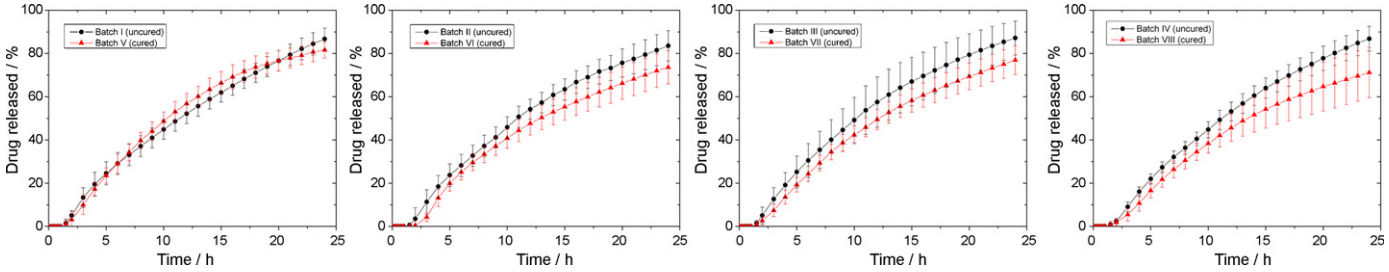

Fig. 8. Average dissolution profiles of 10 pellets (cured and uncured) from each batch. Results from the similarity tests indicated that the drug release curves of the cured pellets were similar to that of the uncured pellets.

for a coarse surface did not happen at equal rates. The film coating growth on the peaks was much faster than that in the valley resulting in extensive thickness variation over the pellet surface (Fig. 7). This coating thickness variation was also confirmed with a pellet cross-section image taken with the SEM (Fig. 7).

3.4. The effect of curing

Curing is optionally carried out at the end of the coating process. It aims at promoting further coalescence of the polymer particles in order to eliminate any undesirable changes in the film coating characteristics upon storage that could be attributed to incomplete film coating coalescence during the film coating procedure (Muschert et al., 2009). A study by Shao et al. using nonpareil cores, demonstrated that curing reduced the Kollicoat® SR 30 D film coating permeability to the dissolution medium, which subsequently hindered drug release (Shao et al., 2002). In contrast, Dashevsky et al. showed that curing had no effect on the drug release from pellets coated with a sustained-release film coating formulation containing mainly Kollicoat® SR 30 D (Dashevsky et al., 2005). Moreover, our previous study on tablet film coatings also containing Kollicoat® SR 30 D as the sustained-release polymer indicated that curing at 60 °C for 48 h increased the film coating density and thus reduced the water permeability into the film coating matrix and consequently decreased the drug release rate (Ho et al., in press-a). These different drug release tendencies as a result of curing might also be partially attributed to the differences in the given coating conditions. In the current study, pellets from batches V–VIII were cured at 60 °C for 24 h. Student's *t*-tests were carried out on the terahertz parameters to compare the film coating characteristics of cured and uncured batches of pellets. All *P*-values were above the null-hypothesis level ($\alpha = 0.05$), which indicated that there was no statistically significant difference between cured and uncured batches in the coating properties – coating thickness and surface roughness (Table 2). Once these pellets were imaged with TPI, drug release testing was carried out subsequently. Pellets from batch I and their cured counterparts (pellets from batch V) showed an f_2 value of 76, which indicates that the two average release curves are similar. However, on close examination of all drug release profiles shown in Fig. 8, a trend becomes visible: that drug release tends to slow down upon curing. This is likely to be attributed to further polymer particle coalescence that results in more dense and less permeable film coatings. Interestingly, using the similarity factor test, the average dissolution profiles for batches II–IV were found to be "similar" to the ones from their respective cured counterparts (batches VI–VIII, respectively). The similarity factor tests indicated equivalence between the dissolution curves with f_2 values of 59, 57 and 53 for batches II and VI, batches III and VII and batches IV and VIII, respectively. Thus the results from the f_2 similarity factor test should be ascertained with some caution.

4. Conclusion

In this study, TPI was employed for the first time to non-destructively investigate the effects of film coating thickness, drug layer uniformity and the effect of curing on in vitro drug release from sustained-release coated pellets. The results from the TPI analysis indicated that there were significant differences in film coating thickness, surface roughness and drug layer uniformity, and these results were also confirmed with SEM. In contrast to previous TPI studies on tablets with a sustained-release film coating, the terahertz parameters derived from the film coating were not indicative of the subsequent drug release performance from the pellets investigated in the present study. This might be due to the pre-dominant drug release mechanism was not diffusion through the film coating structure (as it was the case with the sustained-release coated tablets). TPI demonstrated potential in evaluating larger pellets. The technique affords accurate information on the film coating and the internal structures, future technological advances may render the analysis of standard size pellets possible.

Acknowledgements

The authors wish to thank Department of Anatomy and Structural Biology, University of Otago for access to a stereo-microscope. Both Grace Gardner and Fieke Neuman are acknowledged for their assistance in obtaining the stereo-microscopy images.

References

Andersson, M., Holmquist, B., Lindquist, J., Nilsson, O., Wahlund, K.G., 2000. Analysis of film coating thickness and surface area of pharmaceutical pellets using fluorescence microscopy and image analysis. J. Pharmaceut. Biomed. 22, 325–339.

Bechgaard, H., Nielsen, G.H., 1978. Controlled-release multiple-units and single-unit doses – literature-review. Drug Dev. Ind. Pharm. 4, 53–67.

Costa, P., 2001. An alternative method to the evaluation of similarity factor in dissolution testing. Int. J. Pharm. 220, 77–83.

Dashevsky, A., Wagner, K., Kolter, K., Bodmeier, R., 2005. Physicochemical and release properties of pellets coated with Kollicoat® SR 30 D, a new aqueous polyvinyl acetate dispersion for extended release. Int. J. Pharm. 290, 15–23.

Ensslin, S., Moll, K.P., Metz, H., Otz, M., Mäder, K., 2009. Modulating ph-independent release from coated pellets: effect of coating composition on solubilisation processes and drug release. Eur. J. Pharm. Biopharm. 72, 111–118.

Ensslin, S., Moll, K.P., Paulus, K., Mäder, K., 2008. New insight into modified release pellets – internal structure and drug release mechanism. J. Control. Release 128, 149–156.

European Agency for the Evaluation of Medicinal Products, 1999. Note For Guidance on Quality of Modified Release Products: A. Oral Dosage Forms; B. Transdermal Dosage Forms; Section I (Quality). In Unit. H.M.E., EMEA, London.

Fitzgerald, A.J., Cole, B.E., Taday, P.F., 2005. Nondestructive analysis of tablet coating thicknesses using terahertz pulsed imaging. J. Pharm. Sci. 94, 177–183.

Food and Drug Administration, 1997. Guidance for Industry – Dissolution Testing of Immediate Release Solid Oral Dosage Forms. In Services. Food and Drug Administration, Maryland.

Graffner, C., 2006. Regulatory aspects of drug dissolution from an European perspective. Eur. J. Pharm. Sci. 29, 288–293.

Haddish-Berhane, N., Jeong, S.H., Haghighi, K., Park, K., 2006. Modelling film-coat non-uniformity in polymer coated pellets: a stochastic approach. Int. J. Pharm. 323, 64–71.

Heinicke, G., Schwartz, J.B., 2007. Ammonio polymethacrylate-coated diltiazem: drug release from single pellets, media dependence, and swelling behaviour. Pharm. Dev. Technol. 12, 285–296.

Ho, L., Müller, R., Gordon, K.C., Kleinebudde, P., Pepper, M., Rades, T., Shen, Y.-C., Taday, P.F., Zeitler, J.A., 2008. Applications of terahertz pulsed imaging to sustained-release tablet film coating quality assessment and dissolution performance. J. Control. Release 127, 79–87.

Ho, L., Müller, R., Gordon, K.C., Kleinebudde, P., Pepper, M., Rades, T., Shen, Y.-C., Taday, P.F., Zeitler, J.A., in press-a. Monitoring the film coating unit operation and predicting drug dissolution using terahertz pulsed imaging. J. Pharm. Sci., doi:10.1002/jps.21766.

Ho, L., Müller, R., Gordon, K.C., Kleinebudde, P., Pepper, M., Rades, T., Shen, Y.-C., Taday, P.F., Zeitler, J.A., 2009. Terahertz pulsed imaging as an analytical tool for sustained-release tablet film coating. Eur. J. Pharm. Biopharm. 71, 117–123.

Ho, L., Müller, R., Kruger, C., Gordon, K.C., Kleinebudde, P., Pepper, M., Rades, T., Shen, Y.-C., Taday, P.F., Zeitler, J.A., in press-b. Investigating dissolution performance critical areas on coated tablets: a case study using terahertz pulsed imaging. J. Pharm. Sci. , doi:10.1002/jps.21845.

Ho, L., Müller, R., Römer, M., Gordon, K.C., Heinämäki, J., Kleinebudde, P., Pepper, M., Rades, T., Shen, Y.-C., Strachan, C.J., Taday, P.F., Zeitler, J.A., 2007. Analysis of sustained-release tablet film coats using terahertz pulsed imaging. J. Control. Release 119, 253–261.

Johansson, B., Alderborn, G., 2001. The effect of shape and porosity on the compression behaviour and tablet forming ability of granular materials formed from microcrystalline cellulose. Eur. J. Pharm. Biopharm. 52, 347–357.

Malaterre, V., Pedersen, M., Ogorka, J., Gurny, R., Loggia, N., Taday, P.F., in press. Terahertz pulsed imaging, a novel process analytical tool to investigate the coating characteristics of push-pull osmotic systems. Eur. J. Pharm. Biopharm., doi:10.1016/j.ejpb.2008.10.011.

Moore, J.W., Flanner, H.H., 1996. Mathematical comparison of dissolution profiles. Pharmaceut. Technol. 20, 64–74.

Muschert, S., Siepmann, F., Cuppok, Y., Leclercq, B., Carlin, B., Siepmann, J., 2009. Improved long term stability of aqueous ethylcellulose film coatings: importance of the type of drug and starter core. Int. J. Pharm. 368, 138–145.

Nitz, M., Taranto, O.P., 2008. Film coating of theophylline pellets in a pulsed fluid bed coater. Chem. Eng. Process. 47, 1418–1425.

Pickwell, E., Wallace, V.P., 2006. Biomedical applications of terahertz technology. J. Phys. D: Appl. Phys. 39, R301–R310.

Ringqvist, A., Taylor, L.S., Ekelund, K., Ragnarsson, G., Engstrom, S., Axelsson, A., 2003. Atomic force microscopy analysis and confocal Raman micro-imaging of coated pellets. Int. J. Pharm. 267, 35–47.

Rohera, B.D., Parikh, N.H., 2002. Influence of plasticizer type and coat level on Surelease film properties. Pharm. Dev. Technol. 7, 407–420.

Shao, Z.J., Morales, L., Daiz, S., Muhammad, N.A., 2002. Drug release from Kollicoat® SR 30D coated nonpareil beads: evaluation of coating level, plasticizer type, and curing condition. AAPS PharmSciTech (electronic resource), 3.

Shen, Y.C., Taday, P.F., 2008. Development and application of terahertz pulsed imaging for nondestructive inspection of pharmaceutical tablet. IEEE J. Quant. Electron. 14, 1–9.

Shen, Y.C., Taday, P.F., Pepper, M., 2008. Elimination of scattering effects in spectral measurement of granulated materials using terahertz pulsed spectroscopy. Appl. Phys. Lett., 92.

Siepmann, F., Hoffmann, A., Leclercq, B., Carlin, B., Siepmann, J., 2007. How to adjust desired drug release patterns from ethylcellulose-coated dosage forms. J. Control. Release 119, 182–189.

Siepmann, F., Muschert, S., Leclercq, B., Carlin, B., Siepmann, J., 2008. How to improve the storage stability of aqueous polymeric film coatings. J. Control. Release 126, 26–33.

Spencer, J.A., Gao, Z., Morre, T., Buhse, L.F., Taday, P.F., Newnham, D.A., Shen, Y., Portieri, A., Husain, A., 2008. Delayed release tablet dissolution related to coating thickness by terahertz pulsed image mapping. J. Pharm. Sci. 97, 1543–1550.

Strübing, S., Metz, H., Mäder, K., 2007. Mechanistic analysis of drug release from tablets with membrane controlled drug delivery. Eur. J. Pharm. Biopharm. 66, 113–119.

Taday, P.F., Newnham, D.A., 2004. Technological advances in terahertz pulsed systems bring far-infrared spectroscopy into the spotlight. Spectrosc. Eur. 16, 20–24.

Zeitler, J.A., Kogermann, K., Rantanen, J., Rades, T., Taday, P.F., Pepper, M., Aaltonen, J., Strachan, C.J., 2007a. Drug hydrate systems and dehydration processes studied by terahertz pulsed spectroscopy. Int. J. Pharm. 334, 78–84.

Zeitler, J.A., Shen, Y., Baker, C., Taday, P.F., Pepper, M., Rades, T., 2007b. Analysis of coating structures and interfaces in solid oral dosage forms by three dimensional terahertz pulsed imaging. J. Pharm. Sci. 96, 330–340.

Zeitler, J.A., Taday, P.F., Newnham, D.A., Pepper, M., Gordon, K.C., Rades, T., 2007c. Terahertz pulsed spectroscopy and imaging in the pharmaceutical setting – a review. J. Pharm. Pharmacol. 59, 209–223.